J Mater Sci (2011) 46:7384–7392
DOI 10.1007/s10853-011-5699-x

Urea effect on the mechanism of mullite crystallization

L. S. Cividanes · D. D. Brunelli · C. A. Bertran · T. M. B. Campos · G. P. Thim

Received: 4 March 2011 / Accepted: 6 June 2011 / Published online: 16 June 2011

Abstract Mullite is an excellent structural material due to its physical and mechanical properties. In this study, mullite was obtained by the sol–gel process, using silicic acid, aluminum nitrate, and urea. The urea effect was studied by evaluating samples obtained from urea/Al^{3+} ratio equal to 0, 1, and 3. The kinetic study was conducted using the isoconversional, non-isothermal, Flynn–Wall–Ozawa method. The sample prepared without urea, which is the least homogeneous one, formed spinel and α-alumina at 1150 °C, and Al-poor mullite together with α-alumina, at 1200 °C. The Al-poor mullite crystallization process from this sample showed the lowest yield. The sample prepared with urea/Al^{3+} ratio equal to 1, which has an intermediate behavior, formed spinel at 1100 °C, Al-poor mullite at 1150 °C, and α-alumina together with Al-poor mullite at 1250 °C. However, the sample prepared with urea/Al^{3+} ratio equal to 3, the most homogeneous, formed spinel and Al-rich mullite at 1100 °C. This sample formed Al-poor mullite at 1200 °C with the highest yield. Moreover, the sample synthesized without urea showed a higher porosity and a greater amount of hexacoordinated aluminum at 350 °C. All samples showed the same kinetic model, Šesták and Berggren (SB) for Al-poor mullite crystallization. The samples synthesized with urea crystallized mullite through the same kinetic parameters and constant values of the activation energy, but the sample prepared without urea followed different kinetic parameters and values of activation energy which changed over the course of the crystallization.

L. S. Cividanes (✉) · D. D. Brunelli · T. M. B. Campos · G. P. Thim
Instituto Tecnológico de Aeronáutica, Divisão de Ciências Fundamentais, Praça Marechal Eduardo Gomes, 50, Vila das Acácias, São José dos Campos, SP CEP 12.228-900, Brazil
e-mail: lucianac@ita.br

C. A. Bertran
Universidade Estadual de Campinas, Instituto de Química, Departamento de Físico-Química, Cidade Universitária Zeferino Vaz, Barão Geraldo, Campinas, SP CEP 13083-970, Brazil

Introduction

Mullite is a widely studied ceramic material due to its properties, such as: thermal and chemical stability, low density, low thermal conductivity, good thermal shock behavior, and high-creep resistance. The excellent high temperature properties of mullite make it an attractive ceramic material for high temperature mechanical applications [1, 2].

The mullite chemical formula is defined as $Al_{4+2x}Si_{2-2x}O_{10-x}$, where x represents the amount of oxygen vacancies per unit cell, related to the replacement of silicon ions (Si^{4+}) by aluminum ions (Al^{3+}) in the tetrahedral sites of the mullite structure. Mullite is a stable compound when its composition varies from $3Al_2O_3{\cdot}2SiO_2$ (60 mol% Al_2O_3, $x = 0.25$) to $2Al_2O_3{\cdot}SiO_2$ (67 mol% Al_2O_3, $x = 0.40$) [3, 4]. The Al-poor structure (orthorhombic-mullite or *o*-mullite), which has $x = 0.25$, corresponds to a unit cell with the following parameters: $a = 0.76$ nm, $b = 0.77$ nm, and $c = 0.29$ nm. The Al-richer mullite with $x = 0.61$ (77 mol% Al_2O_3) is a metastable phase, it corresponds to an Al-rich (tetragonal-mullite or t-mullite) structure and has cell length $a = b$ [5]. The Al-poor structure has a double peak in the X-ray diffraction at 26° (2θ-CuKα), referring to crystal planes 120 and 210. The Al-rich structure is characterized by a single peak in the X-ray diffraction at 26° (2θ-CuKα) [6]. Spinel is another phase that can appear in the aluminosilicate synthesis,

which has low crystallinity. The spinel phase is slightly richer in alumina and is characterized by broad peaks in X-ray diffraction at 46 and 67° [7, 8].

The mullite crystallization mechanism depends on the atomic-scale homogeneity of silicon and aluminum of the precursor. When the precursor is homogeneous, the mullite crystallization temperature is lower, and the alumina content in the mullite structure is the same as the starting material one. The concentration of chemical species for homogeneous precursor is uniform in all parts of the sample. Therefore, the control of the hydrolysis and condensation rate of the starting materials is very important in order to increase the precursor homogeneity [9, 10]. Otherwise, phase segregation can occur, which not only promotes the crystallization of undesirable phases, such as α-alumina and spinel, but also determines a high mullitization temperature.

The sol–gel process has been used for the synthesis of mullite. One task of the sol–gel method is the difficulty in controlling the hydrolysis and condensation reaction rates of the precursors [11]. The difference in the reactivity of the starting materials used in the sol–gel process can result in the phase segregation prior to mullite crystallization. However, the sol homogeneity level can be controlled by the action of chemical additives, such as carboxylic acids, β-diketones or functional alcohols, which act as chelating agents and modify the precursor reactivity [12, 13]. Some studies [14, 15] have used organic polydentate ligands, like ethylene glycol, in the mullite synthesis by sol–gel process. The authors considered that these organic ligands can control the polymerization step of the starting materials. They mentioned that these ligands can act as a bridge between aluminum and silicon atoms, since the ethoxy group of tetraethylorthosilicate molecule can be easily replaced by the hydroxyl groups of the ligands [14, 15]. In other studies, citric acid and urea were used in the synthesis of mullite [16, 17]. Citric acid can act as a chelator of aluminum ions, controlling the phase segregation during the drying stage [16, 17]. Jaymes and Douy [18] used urea to synthesize mullite precursors, which was maintained at 80–100 °C, to form ammonia and to promote the increase of pH. Then, the co-polycondensation of aluminum and silicon species occurs with the slow release of ammonia [18]. Thim et al. [19] also studied the effect of urea in addition to mullite sol. They found that urea replaced two water molecules in the first coordination sphere of aluminum at room temperature [19]. We showed [20] the difference between mullite precursor gels prepared with urea using water and ethanol as solvent, in which the urea affected the mullite crystallization in a positive way when the precursor was prepared with a large amount of water (colloidal precursors), and that urea had a negative effect when the precursor was prepared in alcohol media (polymeric precursors). That study suggested that the positive effect of urea in colloidal gels is related to its participation in the hydrolysis and condensation steps of aluminum and silicon, preventing the intense phase segregation. It was also suggested that the negative effect in the polymeric precursors occurred due to the competition between aluminum nitrate, silanol, and urea by the small amount of water [20].

As far as we know there are few studies related to the urea effect on the mullite crystallization and none of them studies the effect of urea content on the mechanism of mullite crystallization. In this sense, this study is related to the effect of the urea content in the mullite crystallization kinetics, where both the crystallization path and the kinetic parameters were determined. The Al-poor mullite crystallization kinetic was studied using the iso-conversional, non isothermal, Flynn–Wall–Ozawa method.

Experimental procedures

Preparation of samples

Aluminum nitrate non-ahydrate ($Al(NO_3)_3{\cdot}9H_2O$; Vetec) was used as aluminum source and sodium metasilicate ($Na_2SiO_3{\cdot}5H_2O$; Aldrich) as silicon source. Silicon and aluminum were used in the mullite stoichiometric molar ratio (Al/Si = 3/1). Urea ($CO(NH_2)_2$; Synth) was used in the urea/Al^{3+} ratio equal to 0, 1, and 3, and these samples were named A-0, A-1, and A-3, respectively.

Silica sol dispersions were obtained by passing sodium metasilicate aqueous solutions (20% w/w) through a column containing ion exchange resin (IR120—Dow Corning). Aluminum nitrate and urea were added to silica sol. The resulting solutions were kept at room temperature until gel formation (about 10 days) and were then stored at 80 °C until xerogel formation (about 30 days).

Characterization techniques

The xerogels were calcined at 1000, 1100, 1150, 1200, and 1250 °C for 2 h, at a heating rate of 10 °C/min. Powders fired at 1000 and 1100 °C were ground, sieved and then analyzed in a X-ray diffraction (XRD) equipment, Philips diffractometer, PW 1830/1840 model, using CuKα radiation, and operating at 40 kV and 25 mA. The powder resulting from firing at 1150, 1200, and 1250 °C was ground, sieved, and then solid NaCl (Carlo Erba), 10% (w/w), was added to the obtained material, after the sample calcination and prior to XRD analysis. NaCl was used as an internal standard to determine the relative amount of crystallized mullite. After the powders have been grounded and sieved separately, the homogeneous distribution of

solid NaCl in the crystallized mullite was obtained through the following procedure: manual mixing of powders in a mortar, with the help of a pestle, followed by sieving the powders. This procedure was repeated three times to ensure homogeneity of the powders. Moreover, the X-ray diffractometer used here rotated the specimen holder while the analysis was being conducted, so it scanned a large area of sample. The relative amount of crystallized mullite is determined by taking the ratio between the XRD patterns intensity at 26° (related to mullite peak; $2\theta = 26.2°$; JCPDS 15-0776) and at 31° (related to NaCl peak; $2\theta = 31.7°$; JCPDS 05-0628). As NaCl contents are equal in all samples and the peaks of mullite and NaCl are present in the same patterns (they are submitted to the same experimental conditions), this ratio gives the mullite contents in each sample in relation to the NaCl contents. Dividing each ratio by the higher ratio (the higher sample is A-3 treated at 1250 °C), the relative amount of mullite in relation to sample A-3 can be determined.

The samples were characterized by infrared spectroscopy after heating treatment at 350 °C for 2 h. This study was recorded in a Fourier transform–infrared spectrophotometer (FT–IR) Arid-Zone Model B102, in the range of 3000–400 cm^{-1}, using: accuracy of 4 cm^{-1}, 32 scans and KBr pellet method.

Samples A-0, A-1, and A-3 were fired at 200 °C for 2 h and then analyzed by simultaneous thermogravimetry/derivative thermogravimetry (TG/DTG), from 200 to 1000 °C, at 10 °C/min, with an platinum crucible in a TG equipment 6200 SII, Exstar 6000. The mass amount was 2 mg and the atmosphere was synthetic air.

Xerogels calcined at 500 °C for 2 h, were analyzed in a differential scanning calorimetry (DSC) experiment, DSC/TG LABSYS™, from 500 to 1400 °C, with an alumina crucible in an argon atmosphere. Each sample was thermally treated at 10, 14, and 20 °C/min. The mass amount was 30 mg. These DSC results were used to study the Al-poor mullite crystallization kinetic.

The kinetic calculus was performed using non-isothermal experiments to avoid errors related to the exceeding time necessary to reach the target temperature, which is the main problem of the isothermal experiment [21]. Moreover, further errors are also obtained by forcing an adjustment mechanism of reaction to the experimental data. Reliable kinetic parameters can only be found when there is no dependence on the reaction mechanism, i.e., when model-free methods are used. The model-free methods are better represented by the iso-conversional method, which calculates the activation energy and pre-exponential factor for each conversion fraction [21]. Thus, the iso-conversional non isothermal Flynn–Wall–Ozawa method was used in this article.

Results

Figures 1, 2, and 3 show the X-ray diffraction of samples A-0, A-1, and A-3 calcined at 1000, 1100, 1150, 1200, and 1250 °C for 2 h. Table 1 shows the relative amount of crystallized mullite for the samples calcined at 1150, 1200, and 1250 °C for 2 h. Figure 4 shows the infrared spectra for samples A-0, A-1, and A-3 after being treated at 350 °C for 2 h. Figure 5 shows the TG/DTG curves for samples A-0, A-1, and A-3 fired at 200 °C for 2 h. The experimental DSC curves for samples A-0, A-1, and A-3 at 10, 14, and 20 °C/min are shown in Fig. 6. For further clarification, only the thermal events related to *o*-mullite crystallization (the ones used in the kinetics studies) are shown. The intensity of each curve was normalized regarding its highest value. Figure 7 shows the dependence on the activation energy to the crystallized fraction for each sample.

Discussion

Characterization

Figures 1, 2, 3 show the crystallization temperatures of samples A-0, A-1, and A-3. All samples crystallized spinel at 1000 °C, but only sample A-0 crystallized α-alumina together with spinel at this temperature. The XRD profiles

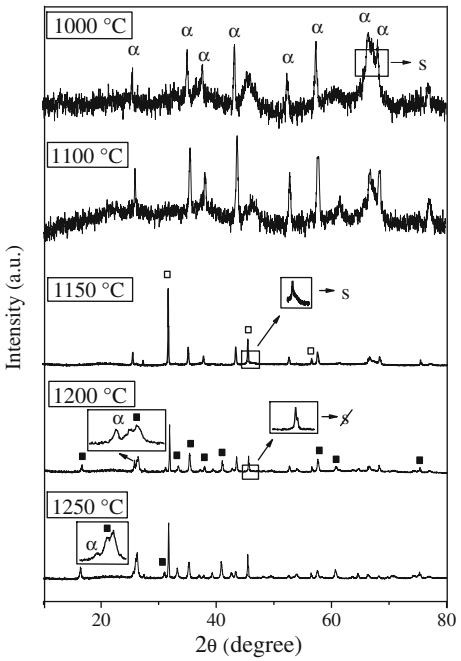

Fig. 1 XRD patterns of sample A-0 fired at 1000, 1100, 1150, 1200, and 1250 °C for 2 h; α α-alumina, *s* spinel, *filled square* mullite, *open square* NaCl, ⊁ spinel not formed

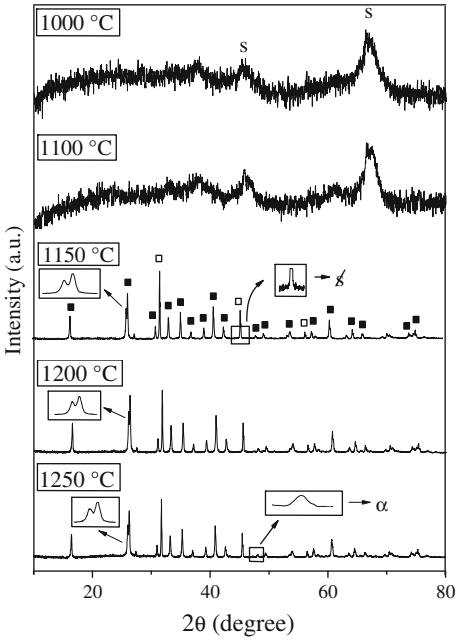

Fig. 2 XRD patterns of sample A-1 fired at 1000, 1100, 1150, 1200, and 1250 °C for 2 h; α α-alumina, *s* spinel, *filled square* mullite, *open square* NaCl, ⊁ spinel not formed

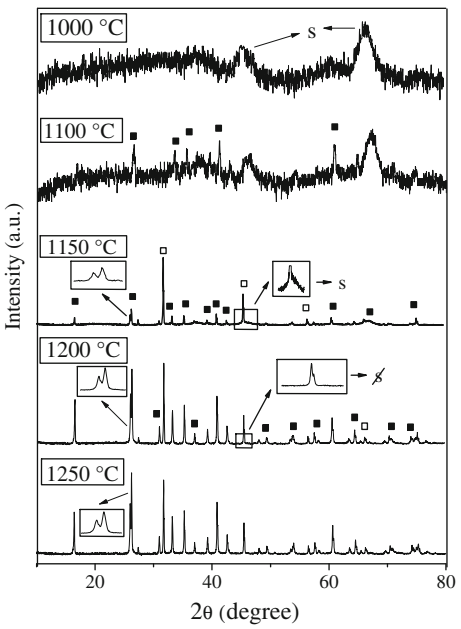

Fig. 3 : XRD patterns of sample A-3 fired at 1000, 1100, 1150, 1200 and 1250°C for 2 h; α α-alumina, *s* spinel, *filled square* mullite, *open square* NaCl, ⊁ spinel not formed

of samples calcined at 1100 °C showed that samples A-0 and A-1 had no change in their crystalline composition, but a remarkable change was observed in sample A-3. This sample crystallized Al-rich mullite together with spinel at 1100 °C. The heat treatment at 1150 °C unchanged the crystalline composition of sample A-0, but *o*-mullite

Table 1 Mullite/NaCl peaks intensity (calculated through XRD patterns) for samples A-0, A-1, and A-3 calcined at 1150, 1200, and 1250 °C

Sample	Relative amount of mullite crystallized		
	1150 °C	1200 °C	1250 °C
A-0	0.00	0.31	0.41
A-1	0.66	0.78	0.80
A-3	0.25	0.82	1.00

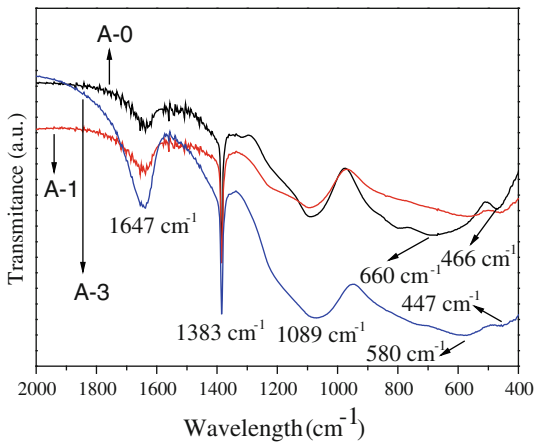

Fig. 4 FT–IR spectra for samples A-0, A-1, and A-3 fired at 350 °C

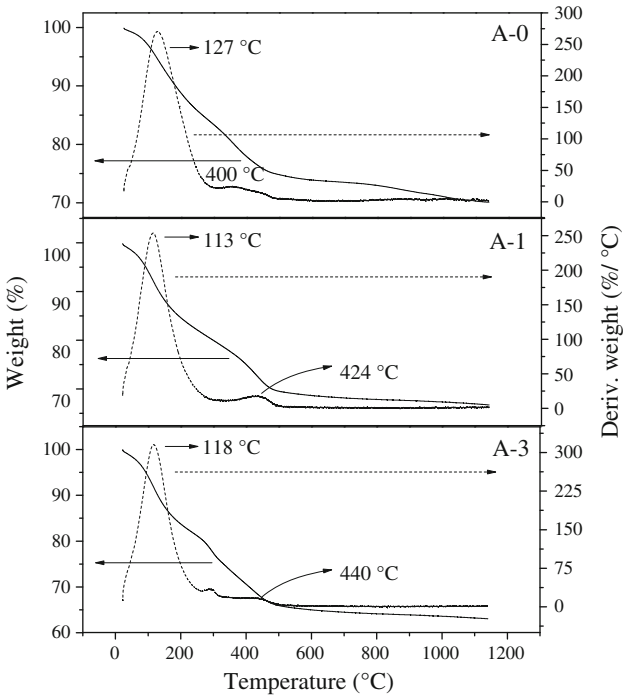

Fig. 5 TG/DTG curves for samples A-0, A-1, and A-3 fired at 200 °C for 2 h

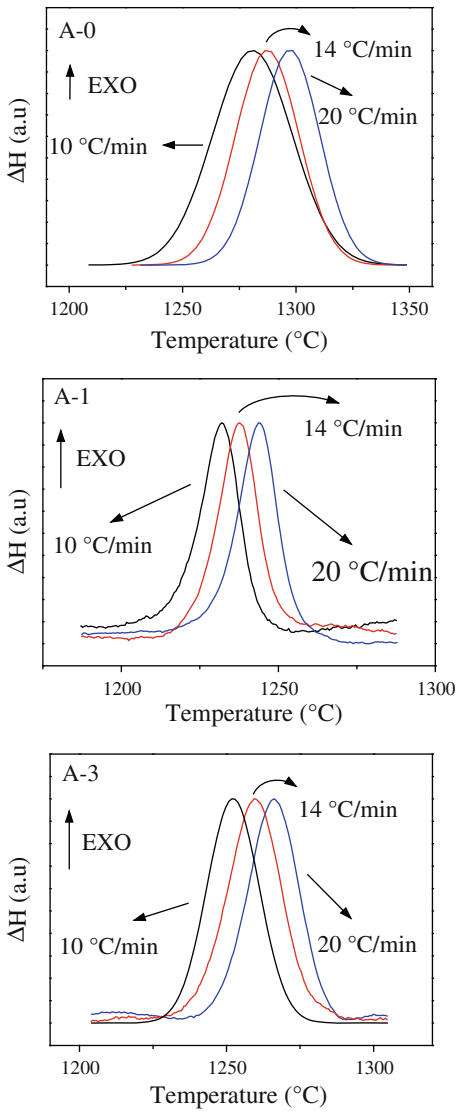

Fig. 6 DSC curves of mullite crystallization for samples A-0, A-1, and A-3

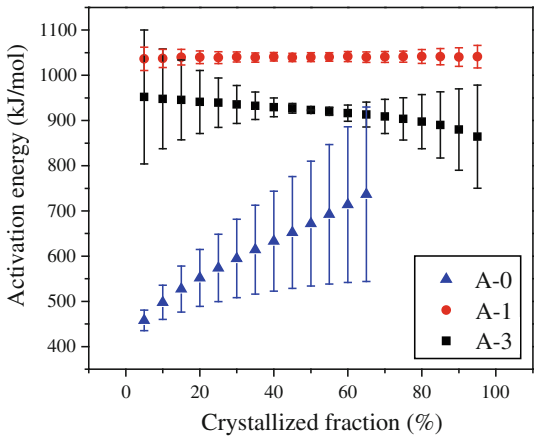

Fig. 7 Plot of activation energy versus crystallized fraction of Al-poor mullite for sample A-0 ($5 \leq \alpha \leq 65\%$), A-1 and A-3

crystallized in samples A-1 and A-3. XRD profile of sample A-3 calcined at 1150 °C showed the presence of spinel and *o*-mullite, and the extinction of the t-mullite crystalline phase. The fraction of *o*-mullite crystallized at 1150 °C (in relation to *o*-mullite crystallized in sample A-3 at 1250 °C) in sample A-1 is higher than the one in sample A-3: 0.66 and 0.25, respectively. After heat treatment at 1200 °C, the crystalline composition of sample A-1 is unchanged, but now *o*-mullite is the only crystalline phase present in sample A-3. With the extinction of the spinel phase in sample A-3 at 1200 °C, one can observe that the amount of *o*-mullite crystallized in sample A-3 increased from 0.25 (at 1150 °C) to 0.82 (at 1200 °C). After sample A-0 treatment at 1200 °C spinel phase also disappeared and *o*-mullite crystallized with a fraction of 0.31, together with α-alumina. At 1250 °C, *o*-mullite was present in all samples, but *o*-mullite was the only crystalline phase in sample A-3, and *o*-mullite was crystallized together with α-alumina in samples A-0 and A-1. Therefore, there were regions rich in Al_2O_3 in samples A-0 and A-1 that led to α-alumina crystallization, where further *o*-mullite would be crystallized only at higher temperatures. Furthermore, mullite crystallized in sample A-0 at 1200 °C with a relative amount of 0.31. Even at 1250 °C the relative amount was too low, about 0.41. Samples A-1 and A-3 crystallize mullite at a much larger relative amount than sample A-0.

Thus, as the *o*-mullite crystallization temperature was 1150 °C for samples A-1 and A-3 and 1200 °C for sample A-0, besides the fact that the samples with urea present a larger amount of crystallized mullite, one can also conclude that urea caused a positive effect in the samples synthesized in this study, increasing the homogeneity of the precursors.

Moreover, the increase in homogeneity caused by the urea addition is directly proportional to the urea content, since sample A-3 crystallized t-mullite at 1100 °C, which is the lowest mullite crystallization temperature, and only sample A-3 leads to crystallization of *o*-mullite as a single phase at 1250 °C.

Table 1 shows that sample A-3 had a lower mullite amount than sample A-1 when they were fired at 1150 °C. However, the opposite occurred at heating treatment at 1200 and 1250 °C, i.e., sample A-3 crystallized larger mullite relative amount than sample A-1 at these temperatures. This difference in the relative amount of mullite can be explained by the differences in the sequence of phases formed during heating treatments. The amount of *o*-mullite present in sample A-3 fired at 1150 °C probably comes from the t-mullite that existed in this sample at 1100 °C, and no longer exists at 1150 °C. Meanwhile, the amount of *o*-mullite of sample A-1 fired at 1150 °C probably comes from the spinel phase that existed in this sample at 1100 °C, and no longer exists at 1150 °C. However, at

1200 °C, the amount of *o*-mullite of sample A-3 is probably the sum of mullite from t-mullite and spinel. In addition, at 1250 °C, sample A-1 formed a lower amount of mullite because part of its material was transformed into α-alumina. Sample A-3 showed no segregation of α-alumina, and thus this sample was able to form larger amounts of mullite.

Figure 4, which shows the infrared spectra for samples A-0, A-1, and A-3 fired at 350 °C for 2 h, also shows the presence of six bands in each sample. These bands are approximately the same for all samples: peaks in 1647, 1383, 1089 cm^{-1}, a broad band in the range of 560–660 cm^{-1}, and a last band at around 450 cm^{-1}. The band assignments are shown in Table 2 [22, 23].

Figure 4 also shows the intensity of the bands assigned to AlO6 group (vibration in the range between 560 and 660 cm^{-1}) and to SiO_4 group (vibration around 450 cm^{-1}). By analyzing the intensity of these two bands in the FT–IR spectra, one can note that both bands have similar relative intensity in the samples with urea (A-1, A-3), unlike the sample without urea (A-0), where the AlO_6 band, in the range between 560 and 660 cm^{-1}, is much higher than the SiO_4 band around 450 cm^{-1}.

Jaymes et al. [9] showed that changes in the coordination number of Si and Al atoms during the mullite crystallization process are related to gel homogeneity. They observed that during *o*-mullite crystallization, the amount of hexacoordinated aluminum cations decreases significantly and the amount of tetracoordinated aluminum cations increases in the same proportion. So, the highest amount of the hexacoordinated aluminum present in the sample A-0 is a strong indication that this sample is less homogeneous than samples A-1 and A-3. These FT–IR results comply with those previously shown by XRD patterns.

Figure 5 shows the TG curves of samples A-0, A-1, and A-3. One can observe that the total mass loss of samples A-0, A-1, and A-3 is 30, 33, and 37%, respectively. These values are consistent with the amount of urea added into each sample: sample A-3 has the highest content of urea and showed the highest value for mass loss, while sample A-0 has the lowest content of urea and showed the lowest value for mass loss.

Table 2 Band locations and assignments for the various vibrational modes for samples A-0, A-1, and A-3 fired at 350 °C for 2 h [22, 23]

Band locations (cm^{-1})	Band assignments
1647	OH
1383	NO_3^-
1089	SiO_4
560–660	AlO_6
450	SiO_4

Figure 5 also shows that the DTG curves of samples A-0, A-1, and A-3 are similar. They show two peaks in common: one of higher intensity at about 120 °C and another smaller and wider at around 420 °C. The peak around 120 °C is a characteristic of the residual water loss from the gel and the crystallization water loss from the aluminum nitrate nonahydrate [24, 25]. The broader peak at around 420 °C in DTG curves occurs due to the thermal decomposition of aluminum nitrate and organic material [26]. Furthermore, Fig. 5 shows that the major loss of mass occurs until about 500 °C for all samples. After this temperature, the mass loss is quite small: sample A-0 lost about 5% of mass and samples A-1 and A-3 lost about 3% of mass.

The increase of the homogeneity caused by the urea addition is possibly related to the interaction between water, urea, and other species in the precursor sol. One of these interactions is probably the formation of the compound $[Al(H_2O)_4{\cdot}(urea)_2]^{3+}$ in mullite precursor sol, as proposed by Thim et al. [19]. The formation of this complex could decrease the condensation rate of the alumina molecules and reduce the formation of the bonds Al–O–Al. Then, an extensive phase segregation of alumina is prevented, and the mullite formation is facilitated. We also observed that the gelation time of the mullite precursor sol is considerably influenced by the urea content, where the gelation time increased when the urea concentration was also increased (not shown here). Thus, urea can also reduce the rate of the Si–O–Si bonds formation, what also avoids an extensive phase segregation of silica. Urea may interact with silanol molecules, blocking the sites responsible for the silanol condensation, preventing silica polymerization. Therefore, the positive effect of the urea addition in the gels prepared with silicic acid, aluminum nitrate non-ahydrate, and water is related to its participation in the alumina and silica condensation stages, preventing the severe phase segregation, then facilitating the mullite formation at lower temperatures and in larger quantities, as it was shown by XRD patterns.

Kinetics calculus

Figure 6 shows the DSC curves for samples A-0, A-1, and A-3, where we can see the exothermic peaks related to *o*-mullite crystallization. *O*-mullite crystallized fractions were determined from each DSC curve (Fig. 6) by Eq. 1. In Eq. 1, α is the crystallized fraction, A_i is the partial area under the peak until a temperature T and A_t is the total area under the DSC peak.

$$\alpha_i = \frac{A_i}{A_t} \tag{1}$$

The activation energy was determined by Eq. 2 [27, 28], where β is the rate heating, T is the absolute temperature

(K), R is the gas constant and E_a^{α} is the activation energy for a given value of α. Plots of log β versus $1/T$ for the crystallized fraction was done (not shown) and taking the slope of the curve the activation energy was graphically determined.

$$\frac{d\log\beta}{d(1/T)} = -\left(\frac{0.457}{R}\right) \times E_a^{\alpha} \quad (2)$$

The values of activation energy are showed in Fig. 7. In this Figure, more than 65% of the data for the crystallization fraction (α) were not plotted for sample A-0 because of the large activation energy errors. For sample A-0, the activation energy increases with the crystallized fraction. This characteristic is related to processes that involve complex mechanisms, frequently represented by more than one step [21, 29]. On the other hand, Fig. 7 also shows that the activation energy is constant with the crystallized fractions for samples A-1 and A-3.

The average values of activation energy were 609, 1040, and 919 kJ/mol for *o*-mullite crystallization of samples A-0, A-1, and A-3, respectively. The average values for samples A-1 and A-3 are higher than the ones for sample A-0. One of the reasons for this lower activation energy for mullite crystallization from sample A-0 could be the formation of highly heterogeneous areas for this sample. As the sample A-0 is composed of a very heterogeneous material, it must have large and small particles of silica and alumina. Within this distribution, there should be few regions with high homogeneity and many regions with very low homogeneity. Therefore, the activation energy calculated refers to *o*-mullite crystallized from a region with high homogeneity. As the amount of samples in this region is too small, the extent of reaction must be also very small. This can be seen in Table 1, which shows that the relative amount of crystallized mullite was only 0.41 at 1250 °C for sample A-0. In other words, this amount is about 1/3 of that one obtained for sample A-3. This small region with high homogeneity could be related to the fact that this sample was the only one that segregated α-alumina prior to mullite formation. Thus, silica is in excess compared to the available alumina to form mullite. So, for being in excess, the silica binds more easily to the alumina present at the interface. The chemical reaction between alumina and silica in excess at this interface leads to mullite crystallization. The interior of the α-alumina particles are not in contact with silica, and thus cannot react to form mullite at this temperature. Therefore, long-distance diffusion is necessary for further mullite crystallization. Tan et al. in 2010 [30], obtained a value of activation energy for the mullite crystallization equals to 741.4 kJ/mol, and attributed this low value of activation energy for an explanation similar to that cited above. They suggested that the low activation energy occurs due to the presence of regions of Si- and Al-rich, then the thermodynamic barrier for mullite nucleation can be reduced for the interface between the Al- and Si-rich regions, resulting in lower activation energy values.

Furthermore, it was shown [20] that the mullite composition for samples A-1 and A-3 fired at 1250 °C is similar, while the mullite composition for the sample A-0 is different. This difference in mullite composition can also explain the difference in the activation energy for samples prepared with and without urea.

The activation energy values found for sample A-0 are in agreement with the results reported by Wei and Rongti [31], which produced mullite from a mixture of α-alumina and quartz, and found activation energy equals to 650 kJ/mol.

The activation energy values found for samples A-1 and A-3 are higher than that value found for mullite crystallization from precursor consisting of silicic acid, aluminum nitrate, and urea, determined by Campos et al. [32]: 730 ± 150 kJ/mol. However, in this occasion, they used the Johnson–Mehl–Avrami–Kolmogorov method (JMAK) for the calculus. On the other hand, the results obtained by Oliveira [33], which used the same method applied here (Flynn–Wall–Ozawa iso-conversional method) for the calculus, showed a value of 1015 ± 272 kJ/mol for the mullite crystallization from mixtures of TEOS, aluminum nitrate, water and ethanol. This activation energy value is in agreement with the values found here for samples A-1 and A-3.

The kinetic model for *o*-mullite crystallization was studied using DSC results for samples treated at 10 °C/min. With Ea values, the curves y(α) and z(α) were calculated by the normalized y(α) and z(α) functions as proposed by Malek [34].

Then, the maximum values of functions y(α) and z(α) (ay and az, respectively) were determined. The model of the crystallization process, Šesták and Berggren (SB), was determined using the values of ay, az, and data from Ref. [35, 36]. SB model is represented by Eq. 3.

$$\frac{d\alpha}{dT} = \frac{A \cdot e^{-E_a/RT}}{\beta} \cdot \alpha^m \cdot (1-\alpha)^n \quad (3)$$

where m and n represent the kinetic exponents from Šesták–Berggren kinetic model.

Once the value of the kinetic exponent n was graphically calculated, the value of the kinetic exponent m was directly obtained. Values of n and m for each sample are shown in Table 3.

Then, the simulated curve $d\alpha/dT$, represented by Eq. 3, can be compared to the experimental one in Fig. 8. By the fact that the simulated and experimental curves are almost overlapping each other, the SB kinetic model, with the

Table 3 Kinetic parameters (p, n, and m) calculated for samples A-0, A-1, and A-3

Sample	p	n	m
A-0	0.50	1.27	0.63
A-1	0.64	1.18	0.75
A-3	0.61	1.18	0.72

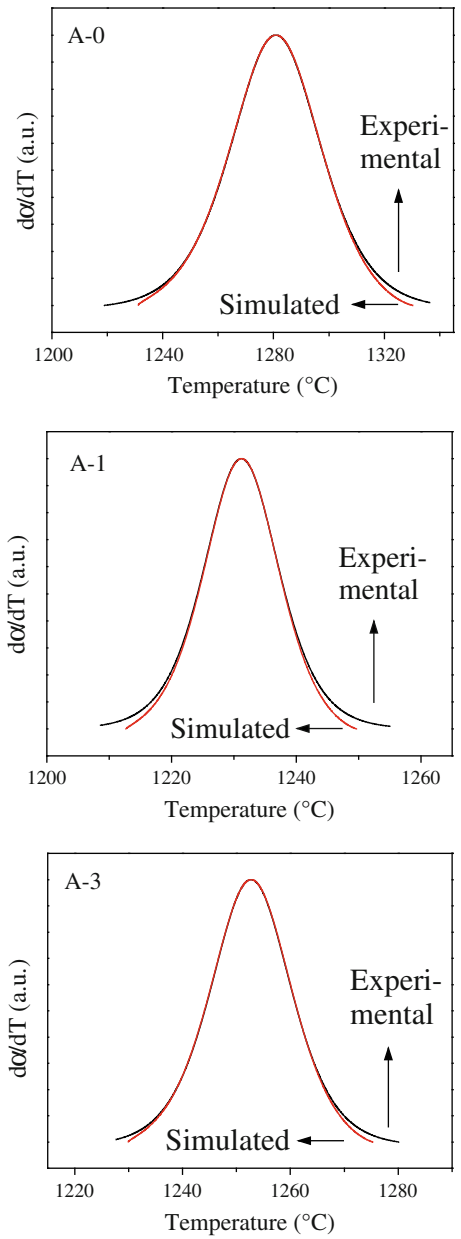

Fig. 8 Experimental and simulated curves of dα/dT versus temperature

determined kinetic exponent, can be considered a good model to describe the *o*-mullite crystallization for samples A-0, A-1, and A-3.

There are some discrepancies between the kinetic exponents for samples A-1 and A-3, n and m, showed in Table 3, in relation to the values for sample A-0. Because the parameters of the SB model are quite similar for samples A-1 and A-3, one can conclude that the crystallization process of *o*-mullite is the same for samples synthesized with urea. Sample A-0 also crystallizes *o*-mullite by the model SB, but it presents a particular crystallization process.

Furthermore, we showed that the activation energy of the sample without urea increases with the increasing of the crystallized fraction, unlike the samples with urea, which have constant activation energies during the course of the reaction. Therefore, the sample without urea crystallized mullite through a complex mechanism that involves several steps, the samples with urea formed mullite by a single step. The values of activation energy are also relatively similar for the samples with urea, and much smaller for the sample without urea. These facts also suggest that the crystallization process of *o*-mullite is quite the same for samples A-1 and A-3, and different for the sample A-0. This similarity in the crystallization process from samples A-1 and A-3, and the discrepancy of the crystallization process from sample A-0, may be explained by differences in the composition of the mullite crystallized from them. Cividanes et al. [20] showed that the composition of mullite formed from the samples A-1 and A-3 at about 1250 °C is 60 and 60.4 mol% in Al_2O_3, respectively, while from the sample A-mullite crystallized with 64.6 mol% in Al_2O_3 at this temperature. Consequently, the samples with urea crystallized Al-poor mullite at 1250 °C with composition close to $3Al_2O_3{\cdot}2SiO_2$, while the sample without urea crystallized Al-poor mullite with composition close to $2Al_2O_3{\cdot}SiO_2$. Moreover, the infrared spectra of samples fired at 350 °C are very similar for samples A-1 and A-3, and a little different for sample A-0, due to the greater amount of hexacoordinate aluminum present in this sample. This difference in the infrared spectra of samples fired at 350 °C may also indicate that the mullite crystallized in samples with urea have similar composition, unlike the mullite crystallized in the sample without urea. As the mullite composition is similar for the samples with urea, and different for the sample without urea, this behavior influences the kinetic parameters of the SB model and the values of activation energy. In other words, the percentages of Al_2O_3 and SiO_2 that composes the mullite directly must influence the parameters of the kinetic model that describes the reaction and the values of activation energy. The fact that the values of activation energy for *o*-mullite crystallization from the sample A-0 are lower than those from the samples A-1 and A-3 may be related to the fact that the activation energy required for crystallizing mullite with composition $2Al_2O_3{\cdot}SiO_2$ is smaller than the activation

energy required for crystallizing mullite with composition $3Al_2O_3{\cdot}2SiO_2$. Wei and Rongti [31] studied the mullite crystallization from a mixture of α-alumina and quartz and mullite was obtained with composition near to $2Al_2O_3{\cdot}SiO_2$. They also observed that the activation energy for this crystallization process was low: about 650 kJ/mol.

Conclusions

Urea addition increases the homogeneity of the samples synthesized with silicic acid, water, and aluminum nitrate non-ahydrate. Samples containing urea crystallized mullite at lower temperatures and in more quantity. Moreover, the mullite obtained from sample without urea showed higher porosity and larger amount of hexacoordinated aluminum at 350 °C, indicating greater heterogeneity of the precursors. The homogeneity of the precursors increased when the urea content also increased, being higher for the sample with urea/Al^{3+} ratio equals to 3.

The samples crystallized Al-poor mullite following the Šesták and Berggren (SB) model for crystallization reaction, with similar kinetic parameters for samples synthesized with urea and different kinetic parameters for samples prepared without urea. The activation energy found for the samples with urea remains constant over the course of the reaction, but do not for the one without urea. The kinetic behavior of *o*-mullite crystallization from samples with urea is similar, whilst they are quite different from that determined for *o*-mullite crystallization from sample without urea. This difference should be related to the content of Al_2O_3 in the mullite structural formula, since the sample without urea leaded to mullite crystallized with composition equals to $2Al_2O_3{\cdot}SiO_2$, while samples with urea led to mullite with a composition equals to $3Al_2O_3{\cdot}2SiO_2$.

Acknowledgements The authors gratefully acknowledge CAPES and FAPESP for financial support and for the collaboration of INPE, AMR-CTA, EEL/USP and IQ-UNICAMP.

References

1. Pascual JZ, Jiménez de Haro MC, Varona I, Justo A, Pérez-Rodríguez JL, Sánchez-Soto PJ (2000) J Mater Chem 10:1409
2. Gerardin C (1994) Chem Mat 6:160
3. Sola ER, Serrano FJ, Torres FJ, Reventós MM, Esteve VJ, Kojdecki MA, Amigó JM, Alarcón J (2006) Cryst Res Technol 41:1036
4. Fielitz P, Borchardt G, Schneider H, Schmucker M, Wiedenbeck M, Rhede D (2001) J Eur Ceram Soc 21:2577
5. Li DX, Thomson WJ (1991) J Am Ceram Soc 74:2382
6. Pask JA (1996) J Eur Ceram Soc 16:101
7. Huling JC, Messing GL (1991) J Am Ceram Soc 74:2374
8. Chakraborty AK (2008) J Mater Sci 43:5313. doi:10.1007/s10853-008-2775-y
9. Jaymes I et al (1996) J Mater Sci 31:4581. doi:10.1007/BF00366355
10. Chakraborty AK (2008) J Mater Sci 43:5376. doi:10.1007/s10853-008-2780-1
11. Niederberger M, Garnweitner G (1996) Chem-Eur J 12:7282
12. Hubert-Pfalzraf LG (1998) Coordin Chem Rev 178:967
13. Schubert U (2005) J Mater Chem 15:3701
14. Mizukami F, Maeda K, Toba M, Sano T, Niwa S-I, Miyazaki M, Kojima K (1997) J Sol-Gel Sci Tech 8:101
15. Stefanescu M, Stoia M, Stefanescu O (2007) J Sol-Gel Sci Tech 41:71
16. Bertran CA, Silva NT, Thim GP (2000) J Non-Cryst Solids 273:140
17. Campos TMB, Cividanes LS, Garcia RBR, Kawachi EY, Thim GP (2008) Efeito do tratamento térmico e do ácido cítrico na cristalização da mulita. In: Proceedings of the 63° Congresso Anual da ABM, Santos, July 28–Aug 1
18. Jaymes I, Douy A (1996) J Eur Ceram Soc 16:155
19. Thim GP, Bertran CA, Barlette VE, Macêdo MIF, Oliveira MAS (2001) J Eur Ceram Soc 21:759
20. Cividanes LS, Campos TMB, Bertran CA, Thim GP (2010) J Non-Cryst Solids (Crystallization 2009) 356:3013
21. Vyazovkin S, Wight CA (1997) Annu Rev of Phys Chem 48:125
22. Schneider H, Komarneni S (2005) Mullite. Wiley-VCH, Weinheim
23. Leivo J et al (2008) J Eur Ceram Soc 28:1749
24. Ban T, Hayashi S, Yasumori A, Okada K (1996) J Eur Ceram Soc 16:127
25. Chakraborty AK (2005) Termochim Acta 427:109
26. Hatakeyama T, Quinn FX (1994) Thermal analysis: fundamentals and applications to polymer science. John Wiley & Sons, New York
27. López-Fonseca R et al (2005) J Therm Anal Calorim 80:65
28. Khawam A, Flanagan DR (2005) Thermochim Acta 436:101
29. Azimi HR (2008) Thermochim Acta 474:72
30. Tan H, Ding Y, Yang J (2010) J Alloys Compd 492:396
31. Wei P, Rongti L (1999) J Mater Sci Eng A271:298
32. Campos AL, Silva NT, Melo FCL, Oliveira MAS, Thim GP (2002) J Non-Cryst Solids 304:19
33. Oliveira TC, Ribeiro CA, Brunelli DD, Rodrigues LA, Thim GP (2010) J Non Cryst Solids (Crystallization 2009) 356:2980
34. Malek J (2000) Termochim Acta 355:239
35. Málek J et al (1992) J Therm Anal 38:71
36. Koga N, Malek J (1996) Thermochim Acta 282–283:69